Evidence for correlated double layers, bipolar structures, and very-low-frequency saucer generation in the auroral ionosphere[a)]

D. L. Newman[b)] and M. V. Goldman
Center for Integrated Plasma Studies, University of Colorado at Boulder, Boulder, Colorado 80309

R. E. Ergun
Laboratory for Atmospheric and Space Physics, University of Colorado at Boulder, Boulder, Colorado 80309

(Received 25 October 2001; accepted 2 January 2002)

Recent observations by the Fast Auroral SnapshoT satellite have provided high-time-resolution measurements of three interrelated phenomena in the downward current region of the auroral ionosphere: Intense parallel electric fields (double layers) localized to tens of Debye lengths; drifting localized bipolar field structures interpreted in terms of electron phase-space holes; and intense quasi-electrostatic whistler emissions (very-low-frequency saucers) originating on the same field lines as the bipolar structures. Numerical simulations and theoretical modeling suggest how these observations may be related. © *2002 American Institute of Physics.* [DOI: 10.1063/1.1455004]

I. INTRODUCTION

A unified picture linking several different nonlinear wave structures and particle phenomena in the downward current region of the auroral ionosphere is now beginning to emerge. Our understanding of this region has been greatly aided by the high-time-resolution capabilities of the FAST (Fast Auroral SnapshoT) satellite[1] coupled with theoretical and numerical modeling efforts. The downward current region is characterized by electrons drifting primarily anti-Earthward, and is thus not associated with the visible aurorae.

In this paper, we consider the interconnection between three types of FAST satellite observations in the downward current region: Localized unipolar parallel electric fields, bipolar parallel electric field pulses, and a class of wave emissions known as "VLF (very-low-frequency) saucers." Each of these observational phenomena can be associated with a basic plasma structure or wave mode, with the strong parallel fields interpreted as electrostatic double layers, the bipolar pulses as the signatures of propagating electron phase-space holes, and the VLF saucers as lower-hybrid and electrostatic whistler waves propagating away from a localized source region.

Bipolar pulses in $E_{\parallel}$ (also referred to as solitary structures) are frequently observed by FAST in the downward current region,[2,3] and have also been observed in a number of other near-Earth space environments.[4–6] An example of a sequence of such pulses[3] is reproduced here in Fig. 1. These bipolar fields have been interpreted as the signature of electron phase-space holes moving past the observing satellite parallel to the Earth's magnetic field. In a one-dimensional (1D) plasma, auroral electron phase-space holes have been modeled[7] as stable Bernstein–Green–Kruskal (BGK) states,[8] with a unipolar potential structure that gives rise to trapped electron orbits. It is the relatively low phase-space density on the lowest-energy trapped orbits that characterizes the object as a "hole." Nevertheless, there is still much to be understood about the dynamics of holes and their interactions in a 1D plasma. A generalization to higher dimensions in a magnetized plasma introduces new behaviors, as discussed below in Sec. III. Electron holes are produced by the saturation of the electron two-stream instability via trapping. Thus, the generation of electron beams is believed to play a key role in the production of phase-space holes in the auroral plasma.

Electrostatic double layers[9,10] are characterized by a localized unipolar electric field, and thus are ideal candidates for the generation of electron beams that can produce holes via the two-stream instability, as has been demonstrated by previous numerical simulations.[11] The first high-time-resolution measurement of a strong unipolar parallel electric field in the downward current region—interpretable as the signature of a double layer—was recently reported.[12] What makes this observation particularly interesting is the existence of a region of intense VLF turbulence on the high potential side (i.e., the side toward which electrons are accelerated). This turbulence region, which was interpreted as consisting of electron holes, is separated by a gap from the double layer field. New 1D Vlasov simulations[13] were able to reproduce many of the features of the observed fields and distributions. These simulation results are reviewed below in Sec. II. A second similar event has recently been measured by FAST[14] in which the VLF turbulence was temporally resolved, thus verifying that it consisted of bipolar fields indicative of the presence of electron holes.

The final class of observations in the downward current region discussed in this paper are VLF saucers,[15–17] which are characterized by "V" or "U" shaped dynamic frequency spectra as illustrated in Fig. 2. The standard interpretation of VLF saucers is that they are lower-hybrid (LH) and electrostatic whistler waves propagating away from a localized source region. The schematic in the lower half of Fig. 2 provides a simple explanation for the characteristic saucer

[a)]Paper CI2 3, Bull. Am. Phys. Soc. **46**, 52 (2001).
[b)]Invited speaker.

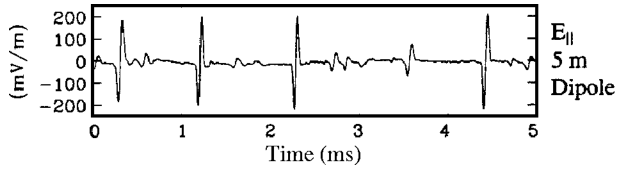

FIG. 1. Example of bipolar electric field pulses in $E_{\parallel}$ from Ref. 3.

shape in the absence of nonidealities such as propagation effects and source motion. The approximate fluid dispersion relation for the LH-whistler branch is

$$\omega^2 = \omega_{\mathrm{LH}}^2 + \omega_e^2 \cos^2 \theta, \tag{1}$$

where θ is the angle between the wave vector $\mathbf{k}$ and $\mathbf{B}_0$. Since the wave group velocity $\mathbf{v}_g$ is perpendicular to $\mathbf{k}$, the minimum frequency (ω_{LH}, which is near the ion plasma frequency) is observed when the satellite is directly above the source region, with the frequency increasing at earlier and later times. The relative location of the source can then be inferred from the shape of the saucer, as explained using a more general model in Ref. 18. High-time-resolution observations of the intense wave activity near the vertices of saucers have been shown[18] to frequently consist of trains of bipolar pulses. Thus, electron holes appear to be associated with the same magnetic field lines as the saucer source regions.

In Sec. III, we discuss the relationship between electrostatic whistlers and electron phase-space holes, as inferred from past two-dimensional (2D) periodic two-stream simulations[19,20] and theoretical analysis.[21,22] Analysis of saucer spectra[17] indicates that the source thickness parallel to $\mathbf{B}_0$ is of order 10 km or less. Thus if the saucers are composed of whistlers generated via interactions with electron holes, the inferred source thickness places constraints on the coupling model, which is discussed in Sec. III D.

The balance of this paper is structured as follows: In Sec. II, we review and expand upon the results of new 1D Vlasov simulations[13] that describe the growth of an electrostatic double layer in an initially field-free plasma at the site of a relatively weak density perturbation. Emphasis is placed upon the interrelation between the double layer and the electron holes generated as a result of interactions of the electron beam accelerated by the double-layer field with background electrons. In Sec. III, the generation of electrostatic whistlers via an instability involving phase-space "tubes" (i.e., a generalization of phase-space holes in a 2D magnetized plasma)[21] is considered as a source mechanism for VLF saucers. Section IV contains concluding remarks.

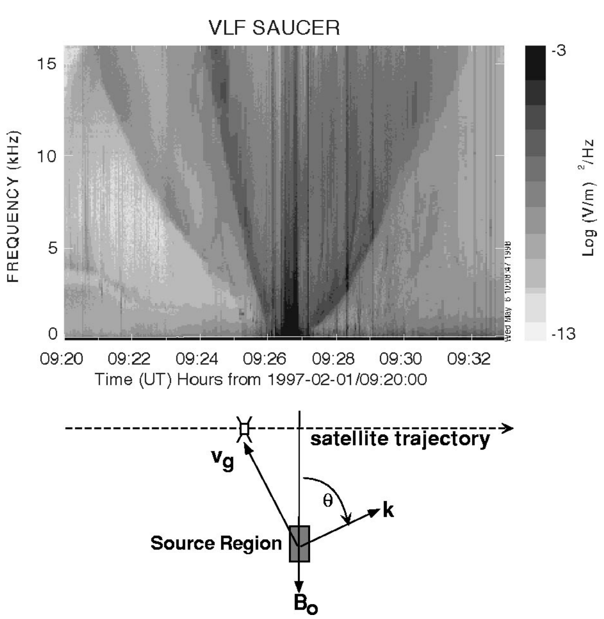

FIG. 2. Top: Example of a VLF saucer as observed by FAST satellite. Bottom: Schematic representation of satellite trajectory relative to the saucer source region.

II. COUPLED EVOLUTION OF DOUBLE LAYERS AND ELECTRON HOLES

In this paper, we do not address issues relating to the origins of auroral currents *per se*, but instead consider the development of localized plasma structures that are driven by currents that are assumed to be preexisting. In this section, we discuss the results of 1D open-boundary Vlasov simulations that follow the evolution of an initially field-free current-carrying plasma in which an initial perturbation in the form of a charge-neutral density depression is introduced. Details of the simulation are presented elsewhere,[13] and only the key features are summarized here.

The simulation domain is initially filled with Maxwellian electrons drifting to the right with velocity u_e nominally equal to the electron thermal velocity v_e, and Maxwellian ions drifting to the left at a nominal velocity $u_i = -v_i$, where $v_i = v_e (T_i m_e / T_e m_i)^{1/2}$, $T_i / T_e = 1$, and $m_i / m_e = 400$. A broad (half-width of $160\lambda_e$) charge-neutral density depression of maximum depth 12.5% is placed in the center of the simulation domain to seed the subsequent evolution (the initial distributions, if homogeneous, would be stable to electron–ion drift instabilities). The initial distributions do satisfy the Langmuir and Bohm criteria of classical double-layer theory.[9] The drift velocities u_e and u_i are adjusted inside the density depression to keep the electron and ion currents independently uniform (i.e., $J_\alpha = n_\alpha u_\alpha$ are independent of x). Related simulations[23] in which u_α is kept uniform instead result in the initial generation of transient Langmuir waves. The simulations discussed here were repeated in a larger simulation box and with a weaker initial density perturbation. The stages of evolution remained relatively unchanged (although there was a significantly longer "startup" period in the latter case) suggesting that the results described here are not significantly biased by limited box size or choice of initial perturbation.

The early stages of evolution follow the course conjectured by Carlqvist:[24] Electrons drifting into the region of lower density on the left side of the initial depression produce a *negative* space-charge layer. Meanwhile, on the right side of the initial depression, a lower-density population of electrons displaces a higher density population and produces

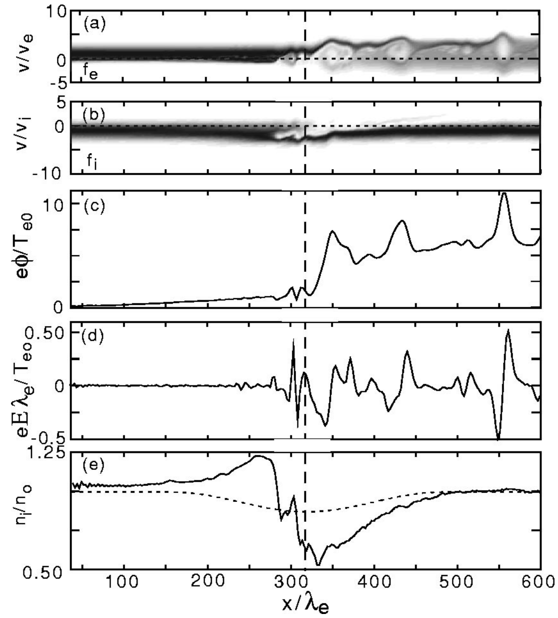

FIG. 3. Simulation distributions and fields at $\omega_e t = 2500$. (a) Electron distribution function; (b) ion distribution function; (c) electrostatic potential; (d) electric field; (e) ion density profile, with dashed curve indicating the initial density depression.

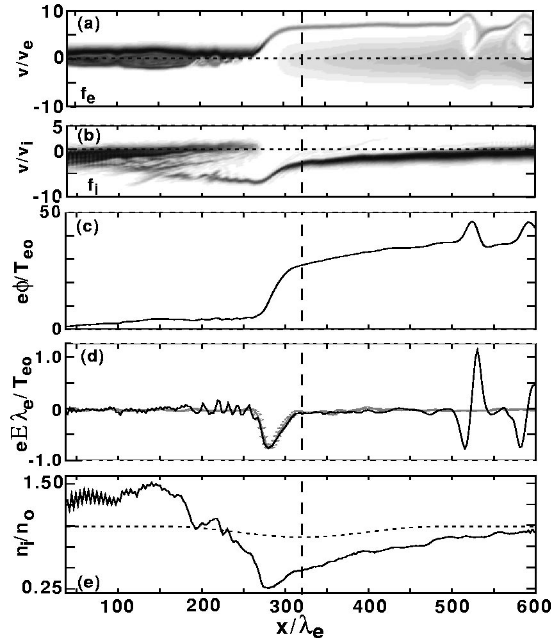

FIG. 4. Same as Fig. 3 except at later time $\omega_e t = 4000$. The gray curve in frame (d) is the DC electric field observed by FAST (Ref. 12) after scaling as described in the text.

a *positive* space-charge layer. The resulting small charge separation is that of an incipient double layer, with an electric field pointing toward the left and thus capable of further accelerating electrons in the direction they were originally drifting. (At these early times, motion of the heavier ions is relatively unimportant.)

Figure 3 shows the evolved distributions and fields at time $\omega_e t = 2500$, which is well into the nonlinear phase of evolution. Electron holes are clearly visible in electron phase-space (a) as are their field signatures: Unipolar potential pulses (c) and bipolar electric field pulses (d). The mean potential is clearly much higher in the right side of the box than in the left, but the electric field in the transition region (x/λ_e between 300 and 350) is quite turbulent. Since there is no isolated monotonically increasing potential ramp, we refer to this structure as a "turbulent double layer." A preliminary analysis of related simulation runs[23] suggests that this turbulence may be due to electron–ion (kinetic Buneman) instabilities. This hypothesis is supported by the perturbations to the ion distribution (b), which has experienced a leftward acceleration by the same fields that accelerate electrons to the right. The ion density has also deepened significantly in the center of the box relative to the initial perturbation (e), which is another characteristic of double-layer formation.

It is important to emphasize that the electron holes are not merely a byproduct of double layer formation. Instead, they appear to play an important role in the evolution of the double layer itself. This feedback mechanism whereby the holes influence the double layer is a consequence of the heating of the embedding plasma through the saturation of the two-stream instability—a process that involves the production of holes via trapping. Because of the importance of electron heating on the high-potential side, the simulation employs "adaptive" boundary conditions on the distribution functions.[13] Thus, the distribution of leftward-moving electrons at the right boundary is adjusted at each time step to reflect the heating of the plasma.

By time $\omega_e t = 4000$, a strong, well-defined (laminar) double layer has developed, as seen in Fig. 4. The potential ramp (c) and unipolar electric field (d) of the double layer are clearly visible at position $x/\lambda_e \approx 280$. The gray curve in frame (d) is the DC parallel electric field measurement from FAST.[12] Values of the simulation parameters $\lambda_e = 5 \pm 2.5$ m and $n_e T_e = 55.3$ eV cm^{-3} were chosen to obtain optimal agreement between the simulation electric field and the data. The density depression has also deepened further (e) with a minimum density of only 25% of the original background density.

An overview of the plasma evolution can be seen in Fig. 5, which is a time history of the electric field over the duration of the simulation run. Following an initial linear growth phase ($\omega_e t \lesssim 500$), a near continuous series of electron holes can be seen moving rightward across the right half of the

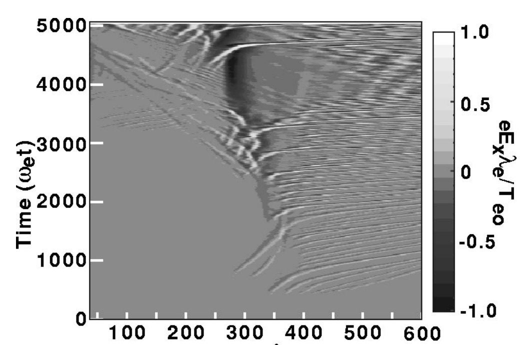

FIG. 5. Time history of the electric field in the interior of the simulation domain.

simulation domain. These holes continue to be generated even when the acceleration region is very turbulent (e.g., $2500 \lesssim \omega_e t \lesssim 3500$) as in Fig. 3. Slower leftward-moving structures also appear to originate from the turbulent region, and can be interpreted as the result of an electron–ion (kinetic Buneman) instability.[23] The laminar double layer of Fig. 4 appears as the narrow dark region near $x/\lambda_e = 300$, which lasts from $\omega_e t \approx 3500$ to $\omega_e t \approx 4500$. This period terminates with a strong disruption caused by a large electron hole that forms on the low-potential side of the double layer. Similar but weaker disruptions can be seen earlier in the run. A preliminary analysis suggests that these holes also originate via an electron–ion instability.[23]

The issue of double-layer disruption is an important one in need of further study. The double layers measured by FAST are observable due to the motion of the double layer relative to the satellite, which is dominated by the drift of the double layer in the ion frame at approximately the ion sound speed.[12] If double layers can be disrupted too easily, the probability of observing one becomes very small. Thus, a goal of future simulations will be to determine how double-layer lifetimes depend on details of the initial distribution functions and other characteristics of the plasma.

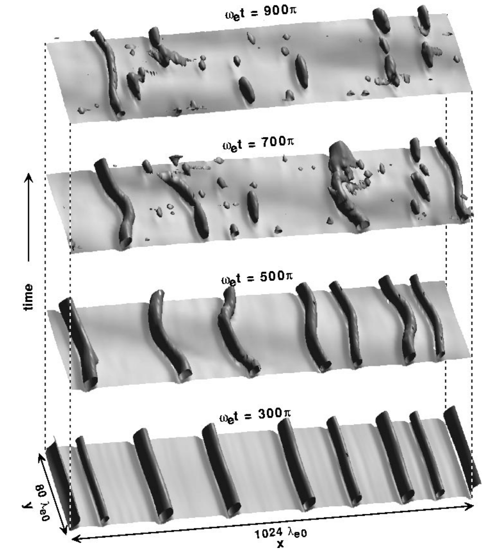

FIG. 6. Isosurfaces in (x, v_x, y) space of f_e at four times (increasing upward) during the evolution of an ensemble of phase-space tubes following the introduction of a monochromatic whistler. The surface corresponding to passing orbits with $v_x > 0$ has been removed to aid visualization.

III. INSTABILITY OF PHASE-SPACE HOLES AND WHISTLER GENERATION

The Vlasov simulations of double-layer formation and electron hole generation discussed above are 1D and, therefore, unable to address the relation of these structures to VLF saucers, which are signatures of obliquely propagating LH and electrostatic whistler waves. However, previous periodic 2D particle-in-cell (PIC) simulations initialized with spatially uniform counterstreaming electron populations in a strong magnetic field $(\Omega_e > \omega_e)$[19,20] showed that electrostatic whistler generation is a byproduct of the nonlinear stages of the 2D two-stream instability. In this section, we will review conclusions drawn from these simulations and a preliminary theory[21,22] for the process producing electrostatic whistler waves. We will then present recent refinements to this theory and suggest how this process may provide a source mechanism for VLF saucer generation.

A. Nonlinear saturation of the two-stream instability in a magnetized plasma

Counterstreaming electron populations saturate via trapping in 1D, with the saturated state consisting of an ensemble of electron phase-space holes. Holes moving at different velocities may interact with one-another by merging, eventually resulting in fewer well-separated holes. In the absence of dynamical ions, isolated electron holes in 1D are essentially stable phase-space structures. However, early unmagnetized 2D and 3D simulations[25] showed that in higher dimensions electron phase-space holes will rapidly dissipate—a conclusion that also follows for sufficiently weak magnetic fields.[26]

Our past 2D simulations of two-stream evolution[19,20] show that the situation is actually more complex for stronger magnetic fields with $\Omega_e > \omega_e$. During the linear phase of the two stream instability, the turbulence is highly incoherent in the direction perpendicular to **B**. However, as the waves grow and electron holes form via trapping, the holes tend to "line up" across **B**, resulting in an ensemble of "tubes" in $x - v_x - y$ phase space. These tubes undergo mergings much as simple holes do in 1D. Eventually though (after several hundred ω_e^{-1}), the tubes begin to develop kinks simultaneous with the appearance of electrostatic waves propagating almost perpendicular to **B** and satisfying the electrostatic whistler dispersion relation of Eq. (1). As the whistlers grow, the kinks become larger and eventually result in the breakup of the tubes into short segments of comparable size parallel and perpendicular to **B**.

The tube-whistler interaction and eventual breakup of phase space tubes is illustrated in Fig. 6, which shows four stages in the evolution of an ensemble of initially straight phase-space tubes as they interact with a monochromatic whistler. The isosurfaces of the electron distribution function in $x - v_x - y$ phase space shown in Fig. 6 are from a 2D magnetized Vlasov simulation (the simulation method is described in Ref. 21). The simulation was initialized with a series of straight tubes formed by uniformally extending across **B** an ensemble of stable holes from a 1D two-stream simulation. This same process was previously used in PIC simulations.[20] However, because of the low noise in Vlasov simulations, we were able to seed the subsequent 2D evolution with a small-amplitude single whistler mode at the fundamental diagonal wavelength of the simulation domain (i.e., at the first nonzero mode in both k_x and k_y). The cylindrical tubes, which are trapped-orbit isosurfaces, are still essentially straight at time $\omega_e t = 300\pi$ following turn-on of the whistler. By time $\omega_e t = 500\pi$, the whistler is clearly visible as a weakly shaded diagonal stripe in the isosurface "sheet" of the passing-electron distribution (underneath the trapped-orbit tubes). The tubes are noticeably kinked at this time, with the displacement parallel to the x axis in phase with the whistler. Up to this point the growth of both the whistler amplitude and kink displacement have been linear, with the phase of the kinks remaining locked to the phase of the whistler, which crosses the simulation box at its linear phase velocity. The final two times show the highly nonlinear phase of evolution where the tubes have become mostly broken up in the y direction, leaving a number of small spheroidal surfaces that enclose regions of low phase-space density.

The aspect ratio of the simulation domain in Fig. 6 is critical to the evolution of the initially straight tubes. We made a number of such runs that were identical in all respects except for the length L_y of the box perpendicular to **B**. The value $L_y=80\lambda_{e0}$ yielded the fastest growth rate, and values significantly different from this yielded no growth at all. The parameter L_y controls the linear frequency of the whistler

$$\omega_w/\omega_e=k_x/(k_x^2+k_y^2)^{1/2}=L_y/(L_y^2+L_x^2)^{1/2}, \tag{2}$$

which suggested that the instability might be due to a resonance between the whistler and some property of the phase-space tubes—specifically, the kinking of the tube—as is discussed next.

B. Vibrations of phase-space tubes

The dynamics of a kinked phase-space tube was investigated numerically by initializing a 2D magnetized Vlasov simulation with a single tube in which a sinusoidal kink was imposed at $t=0$. This was accomplished by setting the initial distribution function to be

$$f_e(x,v_x,y)=f_0(x-\xi(y),v_x), \tag{3}$$

where $f_0(x,v_x)$ is the distribution for an electron hole in a 1D plasma and the displacement $\xi(y)$ takes the form

$$\xi(y)=Re[\xi_0\exp(ik_yy)]. \tag{4}$$

For a given tube cross section (as determined by f_0), the initially kinked tube was found to ''vibrate'' with a frequency ω_v that depended on the kink wave number k_y. For sufficiently small values of k_y these vibrations were essentially undamped, but both the frequency and damping rate increased with increasing k_y.

In the single-tube simulations just discussed, the parallel length L_x of the simulation box was chosen so that there were no whistler modes with ω_w near ω_v, thus eliminating possible resonant tube-whistler interactions. However, when L_x was increased until ω_w from Eq. (2) equaled ω_v, simulations initialized with a kinked tube exhibited tube vibrations of increasing amplitude together with the production of whistlers along the box diagonal, in support of the tube-whistler resonance hypothesis.

A theory for tube vibrations was developed for the specific case where the 1D distribution $f_0(x,v_x)$ took the form of a BGK waterbag electron hole.[21] This theory is based on the fact that a perturbing electric field resulting from the kinking of the tube acts on the trapped electrons (after effectively averaging over the trapping or bounce period) to produce a ''restoring force'' that causes the tube to vibrate like a string under tension. This theory yields good quantitative agreement with single-tube Vlasov simulations over a range of hole sizes and values of k_y, as does a simpler analysis,[22] with one free fitting parameter.

C. Tube–whistler interactions

The simulations discussed in Sec. III A indicated there is a resonant coupling between tube vibrations and electrostatic whistlers. A preliminary theory[21] suggested that tube vibrations could be induced by the whistler electric field at the position of the tube and whistlers in turn could be driven by the perturbed electric field associated with a kinked tube. The first assertion does account for the dominant influence of whistlers on tube dynamics as embodied in the relation

$$(\omega^2-\omega_v^2)\xi=E_{xw}(x_t), \tag{5}$$

where ω is the frequency of the whistler [nominally $\omega_w(k_x,k_y)$], and $E_{xw}(x_t)$ is the whistler electric field evaluated at the mean location of the center of the tube. Further analysis however reveals that the driving of whistlers by tube vibrations is more complex than previously thought. Although a rigorous treatment is beyond the scope of this paper, we will present the main elements of the derivation here.

The electron fluid equations for whistler oscillations in a strongly magnetized plasma with external driving can be written as

$$\partial_t n_w=-\partial_x u_w-\partial_x u_{tw}, \tag{6a}$$

$$\partial_t u_w=-E_{xw}+F_{tw}, \tag{6b}$$

$$n_w=\nabla^2\phi_w, \quad E_{xw}=-\partial_x\phi_w, \tag{6c}$$

where n_w, u_w, ϕ_w, and E_{xw} are the fluid density, velocity, potential, and self-consistent electric field of the whistler, and u_{tw} and F_{tw} represent the influence of the vibrating tube on the whistler. The driving term in the momentum equation F_{tw} needs to incorporate both electric field and pressure gradient terms associated with the vibrating tube. Inclusion of the pressure terms effectively cancels the electric field contribution. Thus, the whistlers cannot arise as a result of electric-field driving, as previously claimed. Instead the dominant driving effect enters via the continuity equation by means of the coupling term u_{tw}. The origin of u_{tw} can be seen in Fig. 7, which shows how electron phase space in the vicinity of a tube evolves over a single tube vibration period. The key feature to notice here is that whereas the centroid of the trapped orbit $(\xi,\dot{\xi})$ executes an elliptical trajectory in phase space, the passing orbits shift horizontally, but not vertically. As a result, when $\xi=0$ and $\dot{\xi}$ is a maximum as in Fig. 7(a), there will be a net flux of electrons moving toward the left, as depicted schematically by the gray arrows. Half a period later (c), when $\dot{\xi}$ is a minimum, the direction of net flux will have reversed. This oscillating flux is the origin of the driving term u_{tw} in Eq. (6a).

The behavior illustrated in Fig. 7 yields the *total* oscillating fluid velocity

$$u_{\mathrm{tot}}(x-\xi)=-v_2(x)\dot{\xi}, \tag{7}$$

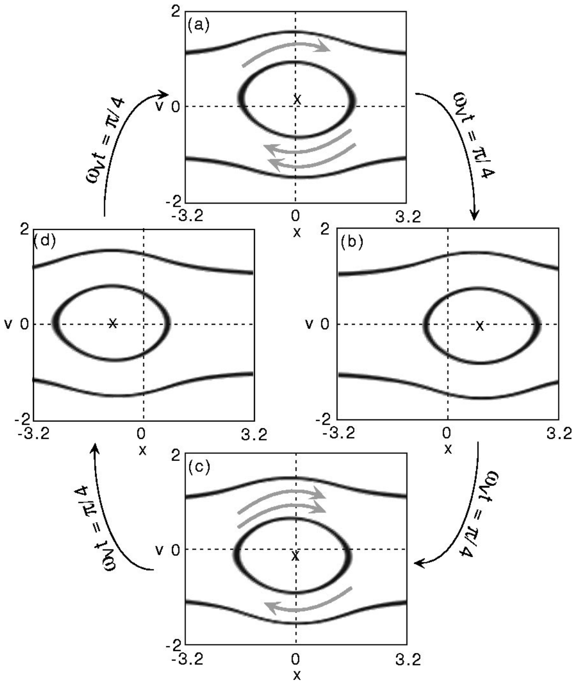

FIG. 7. Passing and trapped waterbag orbits in an $x-v_x$ cross section of a phase-space tube at four times during a single vibration period. Progressing clockwise from top are snapshots when trapped orbit has respectively its maximum upward, rightward, downward, and leftward displacement in phase space. The $\times$ in each frame marks the centroid of the trapped orbit. The gray arrows highlight the asymmetry in the electron flux near the center of the tube in the top and bottom panels.

where $v_2(x)$ is the velocity of the bounding *trapped* orbit of the unperturbed waterbag distribution as defined in Fig. 1 of Ref. 21. The velocity u_{tot} cannot contribute to the driving of whistlers in its entirety, since it must also contribute to the vibration of the tube itself. In other words

$$\partial_x u_{\mathrm{tot}} = \partial_x u_{tw} + \partial_x u_t = \partial_x u_{tw} - \partial_t n_t, \tag{8}$$

where $n_t(x,t)$ is the electron density of the vibrating tube, which undergoes an approximately rigid displacement as can be inferred from the waterbag distributions in Fig. 7 upon integration over v. (The *rigidity* approximation is also discussed in Ref. 21.) The *fluid* velocity u_t is thus related to n_t through the continuity equation. A consequence of rigid density displacement is that

$$\partial_t n_t(x-\xi) \approx -\dot{\xi}\partial_x n_{t0}(x), \quad u_t(x-\xi) = n_{t0}(x)\dot{\xi}, \tag{9}$$

where

$$n_{t0}(x) = v_1(x) - v_2(x) - 1 \tag{10}$$

is the the density of the unperturbed waterbag distribution. Here, $v_1(x)$ is the velocity of the bounding *passing* orbits defined in Fig. 1 of Ref. 21 and the last term on the right side of (10) is the contribution of the homogeneous neutralizing ion background. Combining (7)–(10) yields

$$u_{tw}(x-\xi) = -(v_1(x) - 1)\dot{\xi}. \tag{11}$$

Solving Eqs. (6) for E_{xw} in terms of u_{tw}, and using (11) results in the following equation for resonant driving of whistlers by tube oscillations:

$$(\omega^2 - \omega_w^2) E_{xw}(x_t) = -\omega^2 \omega_w^2 (\langle v_1 \rangle - 1)\xi, \tag{12}$$

where we have used the relation $\dot{\xi} = -i\omega\xi$. Here, ω is the frequency of the tube vibration (nominally ω_v). The following approximations were used in deriving (12): The forcing term F_{tw} in (6b) has been neglected since its influence is normally small compared to that of u_{tw} in (6a). We also use the fact that the parallel whistler wavelength is large compared to the width of the tube. Thus, the small displacement ξ can be neglected so that both x and $x-\xi$ can be replaced by the mean tube position x_t. We also replace v_1 in (11) by its spatial average $\langle v_1 \rangle$ in the periodic simulation domain. Note that $\langle v_1 \rangle - 1$, which determines the strength of the coupling, is positive definite, increases with the size of the hole, and varies as L_x^{-1}. When Eq. (12) and Eq. (5) are combined and solved for ω, as in Ref. 21, there will be positive growth ($Im(\omega) > 0$) provided ω_w and ω_v are sufficiently close to one another.

D. Implications for VLF saucer generation

In order for the tube-whistler instability to be a viable candidate as a source for VLF saucer generation, it is necessary that the whistlers can grow to a large amplitude within the $\lesssim 10$ km range (parallel to $\mathbf{B}$) implied by the saucer spectra. Consistency with this requirement cannot be ascertained through periodic simulations alone. We can, however, construct a semiquantitative model for tube–whistler interactions in an open system.

If a whistler wave packet consisting of a narrow range of wave vectors were to interact with an ensemble of phase-space tubes, coupling should be maximal if the whistlers and tube vibrations *phase lock* to one-another at a single frequency. If this locking occurs, the whistler wave packet will undergo *absolute* growth in the frame of the tubes (i.e., $d\omega/d\mathbf{k} = 0$). If we assume a whistler growth rate $\gamma_w/\omega_e \sim 10^{-2}$ from the 2D PIC simulations[19] together with a drift velocity $v_d \sim 2\times 10^6$ m s^{-1} and plasma frequency $\omega_e \sim 2.5 \times 10^5$ s^{-1} from FAST observations,[12] an approximate growth length $\lambda_g = v_d/\gamma_w \sim 800$ m is found. Thus, 10 km is an adequate distance for over ten e-foldings of the instability.

Once the tubes have been broken up into small structures perpendicular to $\mathbf{B}$, the whistlers are free to propagate at their linear group velocity. At this time, the multiple Fourier components presumed locked to a single frequency during linear growth, which can span a range in $k_\parallel$ and $k_\perp$, will decouple. Thus, each mode will assume its linear frequency according to dispersion relation (1), which is necessary to produce the characteristic saucer spectrum.

IV. CONCLUSIONS

The model developed in this paper consists of two stages: First—as suggested by 1D open-boundary simulations—a double layer forms at the site of a density perturbation in a current-carrying auroral plasma. The generation of phase-space holes is a natural consequence of the double layer and, in fact, appear to play an important role in the development of the double layer itself. Second—as suggested by 2D periodic simulations—phase-space tubes, which are a generalization of phase-space holes in higher dimensions, are subject to a kinking instability through coupling to electrostatic whistlers, which are also driven unstable through this process. These whistlers are potentially the source for observed VLF saucers. Of course, one cannot preclude alternative scenarios for saucer generation. For example, whistlers (and other oblique wave modes) might be produced directly at the site of the double layer. Discrimination between different theories necessarily awaits future simulations with the combined elements of our present simulations: Specifically, 2D open boundary simulations of sufficient spatial extent to allow production of phase space holes in conjunction with a double layer as well as subsequent coupling to electrostatic whistlers. Whatever future studies reveal, the mutual interactions of double layers, electron phase-space holes, and electrostatic whistlers will likely be an important element.

ACKNOWLEDGMENTS

This research was supported by grants from NSF (ATM-9802209), NASA (NAG5-9026), and DOE (DE-FG03-98ER54502). Computations were performed at NCAR, the Advanced Computing Laboratory at LANL, and at NERSC.

[1] C. W. Carlson, R. Pfaff, and J. G. Watzin, Geophys. Res. Lett. **25**, 2013 (1998).
[2] R. E. Ergun, C. W. Carlson, J. P. McFadden, F. S. Mozer, G. T. Delory, W. Peria, C. C. Chaston, M. Temerin, I. Roth, L. Muschietti *et al.*, Geophys. Res. Lett. **25**, 2041 (1998).
[3] R. E. Ergun, C. W. Carlson, J. P. McFadden, F. S. Mozer, L. Muschietti, I. Roth, and R. J. Strangeway, Phys. Rev. Lett. **81**, 826 (1998).
[4] H. Matsumoto, H. Kojima, T. Miyatake, Y. Omura, M. Okada, and M. Tsutsui, Geophys. Res. Lett. **21**, 2915 (1994).
[5] J. R. Franz, P. M. Kintner, and J. S. Pickett, Geophys. Res. Lett. **25**, 1277 (1998).
[6] S. D. Bale, P. J. Kellogg, D. E. Larson, R. P. Lin, K. Goetz, and R. P. Lepping, Geophys. Res. Lett. **25**, 2929 (1998).
[7] L. Muschietti, I. Roth, R. E. Ergun, and C. W. Carlson, Geophys. Res. Lett. **26**, 1093 (1999).
[8] I. B. Bernstein, J. M. Greene, and M. D. Kruskal, Phys. Rev. **108**, 546 (1957).
[9] L. P. Block, Astrophys. Space Sci. **55**, 59 (1977).
[10] H. Schamel, Phys. Rep. **140**, 161 (1986).
[11] N. Singh, Geophys. Res. Lett. **27**, 927 (2000).
[12] R. E. Ergun, Y.-J. Su, L. Andersson, C. W. Carlson, J. P. McFadden, F. S. Mozer, D. L. Newman, M. V. Goldman, and R. J. Strangeway, Phys. Rev. Lett. **87**, 045003 (2001).
[13] D. L. Newman, M. V. Goldman, R. E. Ergun, and A. Mangeney, Phys. Rev. Lett. **87**, 255001 (2001).
[14] L. Andersson, R. E. Ergun, D. Newman, J. P. McFadden, and C. W. Carlson, ''Characteristics of parallel electric fields in the downward current region of the aurora,'' Phys. Plasmas (to be published).
[15] D. A. Gurnett, J. Geophys. Res. **71**, 5599 (1966).
[16] R. L. Smith, Nature (London) **224**, 351 (1969).
[17] H. G. James, J. Geophys. Res. **81**, 501 (1976).
[18] R. E. Ergun, C. W. Carlson, J. P. McFadden, R. J. Strangeway, M. V. Goldman, and D. L. Newman, Geophys. Res. Lett. **28**, 3805 (2001).
[19] M. V. Goldman, M. M. Oppenheim, and D. L. Newman, Geophys. Res. Lett. **26**, 1821 (1999).
[20] M. M. Oppenheim, D. L. Newman, and M. V. Goldman, Phys. Rev. Lett. **83**, 2344 (1999).
[21] D. L. Newman, M. V. Goldman, M. Spector, and F. Perez, Phys. Rev. Lett. **86**, 1239 (2001).
[22] D. L. Newman and M. V. Goldman, Phys. Scr., T **89**, 76 (2001).
[23] M. V. Goldman, D. L. Newman, and R. E. Ergun, ''Phase-space holes due to electron and ion beams accelerated by a current-driven potential ramp,'' Nonlin. Proc. Geophys. (to be published).
[24] P. Carlqvist, Cosm. Electrodyn. **3**, 377 (1972).
[25] R. L. Morse and C. W. Nielson, Phys. Rev. Lett. **23**, 1087 (1969).
[26] L. Muschietti, I. Roth, C. W. Carlson, and R. E. Ergun, Phys. Rev. Lett. **85**, 94 (2000).